Uporaba daljinskega zaznavanja pri oceni tveganja za sušo s spektralnimi indeksi in modeliranjem: študija primera v severnem delu osrednjega Vietnama

Application of remote sensing in drought risk assessment using spectral indices and modelling: a case study in North Central Vietnam

Le Hung Trinh, Thi Thu Trang Tran, Van Phu Le, Thi Phuong Thao Do, Thi Hanh Tong

UDK: 528.8:551.577.38(597)
Klasifikacija prispevka po COBISS.SI: 1.01
Prispelo: 15. 8. 2025
Sprejeto: 26. 1. 2026

DOI: https://doi.org/10.15292/geodetski-vestnik.2026.02.213-229
SCIENTIFIC ARTICLE
Received: 15. 8. 2025
Accepted: 26. 1. 2026

IZVLEČEK

Suša je ena najhujših okoljskih nevarnosti, saj močno vpliva na kmetijstvo, ekosisteme in razpoložljivost vode, zlasti v ranljivih regijah, kakršna je osrednji Vietnam. V pričujoči študiji se ocenjuje tveganje za sušo v provinci Quang Tri v obdobju 2016–2025 na podlagi posnetkov površinske odbojnosti Sentinel-2 in večindeksnega pristopa daljinskega zaznavanja. Pet indeksov, ki so pomembni za sušo, med njimi NDVI, NDWI, EVI, MSI in SAVI, je bilo izračunanih in integriranih z uteženo prekrivno analizo na platformi Google Earth Engine. Vsakemu indeksu je bila dodeljena utež na podlagi njegovega prispevka k značilonstim suše: NDVI (30 %), NDWI (25 %), EVI (20 %), MSI (15 %) in SAVI (10 %). Dobljeni zemljevidi tveganja za sušo so bili razvrščeni v pet stopenj. Analiza je pokazala, da je prevladovala blaga suša, ki je letno pokrivala med 60,14 % in 70,16 % celotne površine. Zmerna suša se je gibala od 15,41 % do 20,76 %, huda suša pa je dosegla vrhunec na 476,96 km² (9,84 %) leta 2020. Ekstremna suša, ki je bila sicer manj pogosta, je bila najhujša leta 2020 in je prizadela 187,35 km² (3,87 %). Nasprotno pa so se območja brez suše sčasoma zelo zmanjšala in leta 2023 dosegla minimum 111,46 km² (2,30 %). Ugotovitve kažejo na vse resnejše suše in prostorsko nesorazmerje, zlasti na gorskih in obalnih območjih. Pristop se je pokazal kot učinkovit za obsežno spremljanje suše in podpira lokalne oblasti pri izvajanju ciljno usmerjenih strategij za blaženje in prilagajanje podnebnim spremembam.

KLJUČNE BESEDE

suša, Sentinel-2, utežena prekrivna analiza, večindeksni prostop, provinca Quang Tri

ABSTRACT

Drought is one of the most pressing environmental hazards, severely impacting agriculture, ecosystems, and water availability, especially in vulnerable regions such as Central Vietnam. This study assessed drought risk in Quang Tri province during the period from 2016 to 2025 using Sentinel-2 surface reflectance imagery and a multi-index remote sensing approach. Five drought-related indices including NDVI, NDWI, EVI, MSI, and SAVI were calculated and integrated using a Weighted Overlay Analysis on the Google Earth Engine platform. Each index was assigned a weight based on its contribution to drought characterization: NDVI (30%), NDWI (25%), EVI (20%), MSI (15%), and SAVI (10%). The resulting drought risk maps were classified into five levels. The analysis showed that mild drought dominated, covering between 60.14% and 70.16% of the total area annually. Moderate drought ranged from 15.41% to 20.76%, while severe drought reached a peak of 476.96 km² (9.84%) in 2020. Extreme drought which though less frequent was most severe in 2020, affecting 187.35 km² (3.87%). In contrast, non-drought areas dropped significantly over time, reaching a minimum of 111.46 km² (2.30%) in 2023. The findings highlight increasing drought severity and spatial disparity, particularly in upland and coastal zones. This approach proves effective for large-scale drought monitoring and supports local authorities in implementing targeted mitigation and climate adaptation strategies.

KEY WORDS

Drought, Sentinel-2, multi-index, Weighted Overlay Analysis, Quang Tri province

1 INTRODUCTION

Drought represents a complex natural hazard that evolves gradually and persists over extended periods (Maybank et al., 1995; Wilhite, 2000). It primarily arises from prolonged precipitation deficits and/or excessive evapotranspiration (Mishra and Singh, 2010; Hollins and Dodson, 2013). Depending on the affected components of the hydrological and socio-environmental systems, droughts are commonly categorized into meteorological, hydrological, agricultural, and socioeconomic types (Van Loon, 2015; Wang and Wang, 2025). As one of the most severe climate-induced phenomena, it exerts substantial impacts on food security, livelihoods, and ecosystem stability, particularly in regions highly dependent on agricultural production and natural water resources (Agele, 2021; Orimoloye et al., 2022; Bogale and Erena, 2022). Recent evidence indicates an increasing frequency and intensity of drought events under global climate change, emphasizing the necessity for advanced drought risk assessment and early warning systems to support mitigation and adaptation strategies (Pulwarty and Sivakumar, 2014; Vogt et al., 2018).

In this setting, remote sensing has emerged as an effective technique for tracking drought dynamics at both spatial and temporal dimensions (Trinh & Vu, 2019; Diaz et al., 2020; Kumar et al., 2024). Compared to traditional ground-based observations, which are typically scarce, costly, or delayed, satellite-based remote sensing delivers timely, consistent, and spatially extensive data, enabling the detection of vegetation stress, surface moisture deficits, and land degradation trends (Mullapudi et al., 2023). There are numerous remote sensing-based methods for assessing drought risk, ranging from simple index-based approaches to complex artificial intelligence algorithms (Gholinia and Abbaszadeh, 2024). Traditional single-index methods are widely used because of their simplicity and direct relationship to vegetation vigor and surface moisture. These indices are computationally efficient and simple to interpret, making them ideal for rapid assessments, particularly in data-scarce regions. However, single-index techniques frequently fail to reflect the multidimensional nature of drought and might yield misleading results in places with dense vegetation or variable land cover (Ghosh et al., 2024).

To overcome these limitations, multi-index integration methods have gained popularity (Baik et al., 2022). By combining multiple vegetation and moisture indicators, researchers can generate a more comprehensive picture of drought conditions. Techniques like Principal Component Analysis (PCA), fuzzy logic, Weighted Overlay Analysis (WOA) allow for spatially explicit classification of drought risk zones based on the relative contribution of each index (Arabzadeh et al., 2016; Hodasová et al., 2025). While these methods provide more robust and interpretable results, they rely heavily on the proper selection and weighting of input indices (Kim et al., 2021). Recent advancements in machine learning (ML) and deep learning (DL) have further enhanced drought monitoring capabilities (Crocetti et al., 2020; Prodhan et al., 2021; Tyagi et al., 2022). ML algorithms such as Random Forest and Support Vector Machines can model complex, nonlinear relationships between remote sensing features and ground-based drought observations (Prodhan et al., 2022). Deep learning techniques like Convolutional Neural Networks (CNNs) and Long Short-Term Memory (LSTM) networks offer powerful tools to capture spatial and temporal patterns in large-scale satellite datasets (Moskolaï et al., 2021). Despite their high accuracy, these data-driven approaches require substantial training data, computational resources, and expertise, and their black-box nature may limit interpretability for operational decision-making (Pelletier et al., 2019; Wang et al., 2022). Compared with PCA, fuzzy logic, and ML models, the WOA offers a transparent, interpretable, and data-efficient solution suitable for regions with limited ground data such as Vietnam and Southeast Asia. It provides a practical and replicable framework for integrating multiple indices to identify drought-prone areas and support local adaptation planning.

Over the past decade, drought in Quang Tri has become more frequent and severe, driven by climate change, deforestation, and intensive land use practices. These drought events have caused significant declines in agricultural productivity, water shortages for irrigation and domestic use, and degradation of natural ecosystems. Despite being an agriculturally important area, the province lacks a systematic and spatially explicit drought risk assessment framework that integrates satellite data and modern analytical methods (Tuan et al., 2014). Given these challenges, Quang Tri serves as a representative case for applying remote sensing-based drought monitoring approaches. Its varied landscape, climate vulnerability, and socio-economic reliance on agriculture underscore the need for detailed, long-term drought risk mapping to support adaptive land and water management strategies.

This study adopts a multi-index approach based on Sentinel-2 imagery to assess drought risk in Quang Tri province, Vietnam, during the period from 2016 to 2025. Five key indices including NDVI, NDWI, MSI, EVI, and SAVI were calculated and integrated using Weighted Overlay Analysis on the Google Earth Engine platform. The resulting drought risk map classifies the area into five levels, from very low to very high. This method offers a balance between analytical rigor and practical applicability, supporting local resource management and climate adaptation efforts.

2 MATERIALS AND METHODOLOGY

2.1 Study area and Materials

Study area. Quang Tri province is located in the North Central Coast of Vietnam, is one of the regions most affected by drought due to its transitional geographic location and complex topography (Figure 1). The province encompasses coastal lowlands, midlands, and mountainous terrain, making it highly sensitive to both climatic and hydrological variability. With a tropical monsoon climate, Quang Tri experiences distinct wet and dry seasons; however, rainfall is often unevenly distributed both spatially and temporally. In particular, the western districts such as Huong Hoa and Dakrong frequently suffer from prolonged dry periods, while the eastern lowlands face increasing pressure on water resources during the dry season.

Materials. Sentinel-2 data is product of the European Space Agency's Copernicus program, provides high-quality satellite photography of the Earth's surface, supporting a wide range of applications in environmental research, agriculture, disaster monitoring, and urban planning (ESA, 2025). The Sentinel-2 constellation consists of two primary satellites, Sentinel-2A and Sentinel-2B, which were launched in 2015 and 2017, respectively, and are equipped with the MultiSpectral Instrument (MSI), which collects data from 13 different spectral bands (Table 1). This enables extensive investigation of surface features like as land, vegetation, water, and urban areas with spatial resolutions ranging from 10 m to 60 m, depending on the spectral band (ESA, 2025). Sentinel-2 can cover a large area of 290 km x 290 km every scan and has a revisit period of about 5 days, which allows it to monitor changes in the environment almost instantly. Sentinel-2 data has proven to be valuable in many fields, from monitoring crop growth and plant health to assessing water resources and analyzing land use and urban expansion. In particular, Sentinel-2 data is a crucial instrument for tracking the effects of urbanization and climate change, allowing decision-makers to act quickly and intelligently (ESA, 2013).

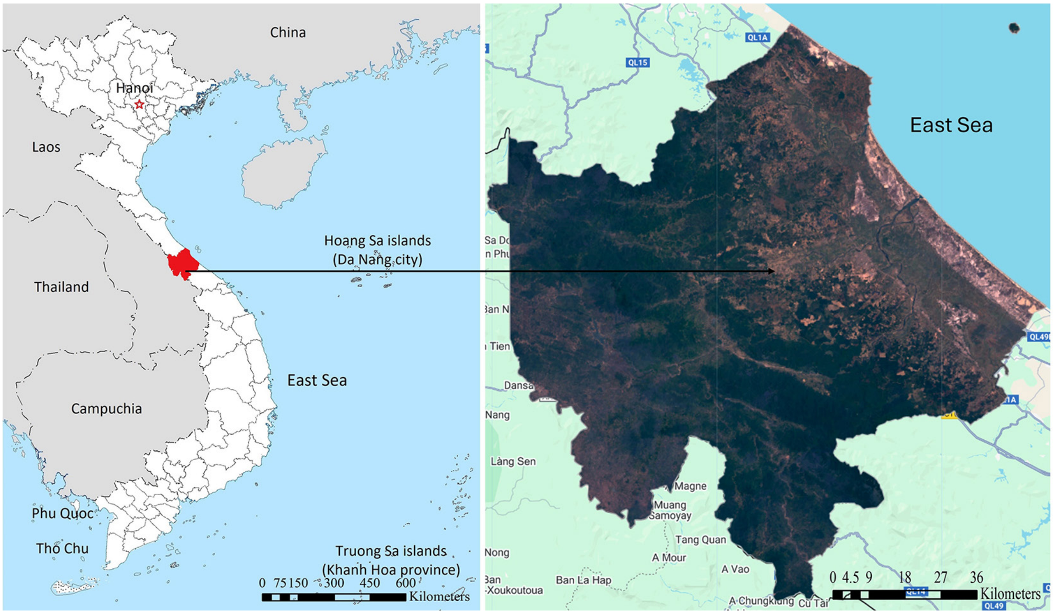

Figure 1: Geographic location of Quang Tri province, Vietnam

Table 1: Sentinel-2 bands characteristics (Google Earth Engine, 2025)

Bands	Description	Central Wavelength S2A (nm)	Central Wavelength S2B (nm)	Resolution (m)
1	Coastal Aerosol	443.9	442.3	60
2	Blue	496.6	492.1	10
3	Green	560	559	10
4	Red	664.5	665	10
5	Vegetation Red Edge 1	703.9	703.8	20
6	Vegetation Red Edge 2	740.2	739.1	20
7	Vegetation Red Edge 3	782.5	779.7	20
8	NIR	835.1	833	10
9	Narrow NIR	864.8	864	20
10	Water Vapour	945	943.2	60
11	SWIR-Circus	1375.5	1376.9	60
12	SWIR	1613.7	1610.4	20
13	SWIR	2202.4	2185.7	20

In this study, ten Sentinel-2 MSI scenes from the period 2016 - 2025 were used to calculate drought indices, which were then applied to delineate drought risk zones in Quang Tri Province. The Sentinel-2 MSI satellite imagery used in this study (in a true color composite with red (Band 4), green (Band 3), and blue (Band 2) bands) is presented in Figure 2.

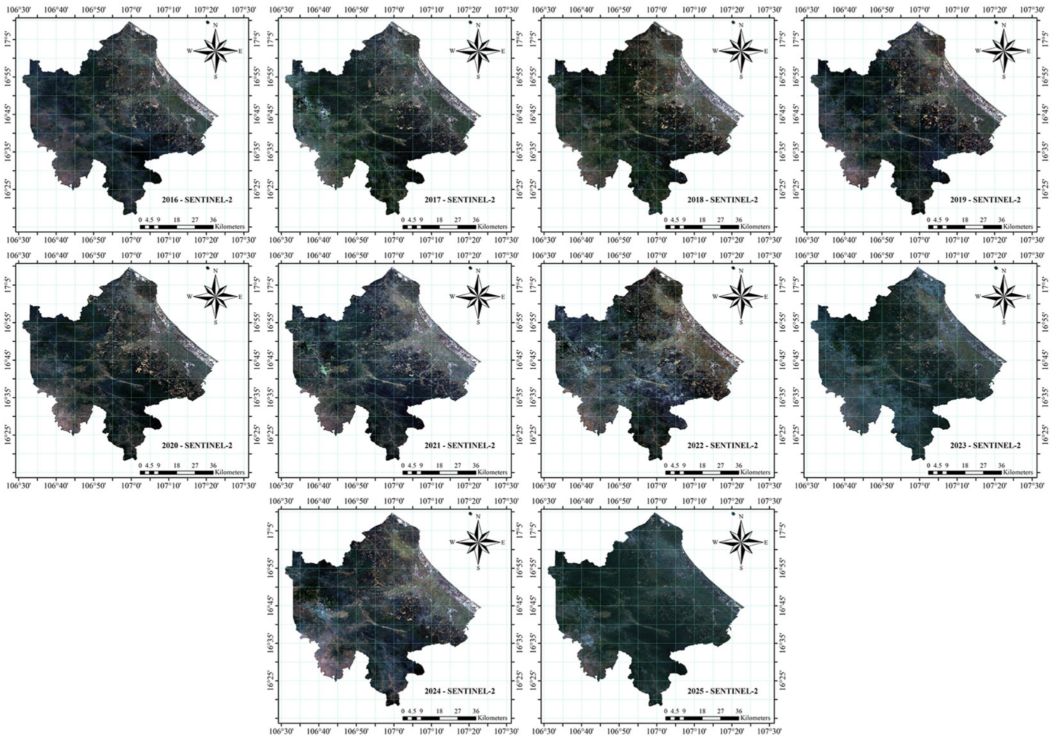

Figure 2: Sentinel-2 images of the study area during the period 2016-2025

2.2 Methodology

The drought risk classification process using Sentinel-2 imagery is presented in Figure 3, illustrating a systematic and structured workflow for identifying and analyzing drought-prone areas. The dry season in Quang Tri province occurs from December to April, with low rainfall and high evapotranspiration. Sentinel-2 images from this period were selected for each year between 2016 and 2025 to ensure consistency. About 6 - 10 cloud-free scenes per year were used, totaling roughly 75 image tiles. The study area is mainly covered by tiles 48PWT and 48PXS, and after cloud masking (using QA60 quality assurance band) and mosaicking on Google Earth Engine, around 90 image dates were processed in total. The selection criteria prioritized cloud-free scenes with minimal atmospheric disturbance.

Image preprocessing involved several key steps. First, the spatial extent of Quang Tri province was defined using administrative boundary shapefiles and applied to all images using the *clip()* function to restrict the analysis to the study area. Next, cloud-contaminated pixels were removed using the Sentinel-2 QA60 quality assurance band, in which pixels flagged as cloud and cirrus were masked out through a bitwise operation (bitwiseAnd) combined with the *updateMask()* function. Atmospheric effects and radiometric distortions were minimized by using surface reflectance data, which had already been atmospherically corrected through the Sen2Cor processor (GEE, 2025). A median composite for each year was then generated using the *median()* reducer, which is effective in minimizing the influence of remaining outliers and extreme pixel values caused by atmospheric variability. The resulting annual composites were used as input datasets for drought analysis. This preprocessing workflow ensured high-quality, temporally consistent datasets suitable for calculating vegetation and moisture indices and conducting drought risk assessment. Subsequently, five remote sensing indices commonly used to monitor vegetation condition and surface moisture were computed using band math expressions applied through the expression() function, as summarized in Table 2.

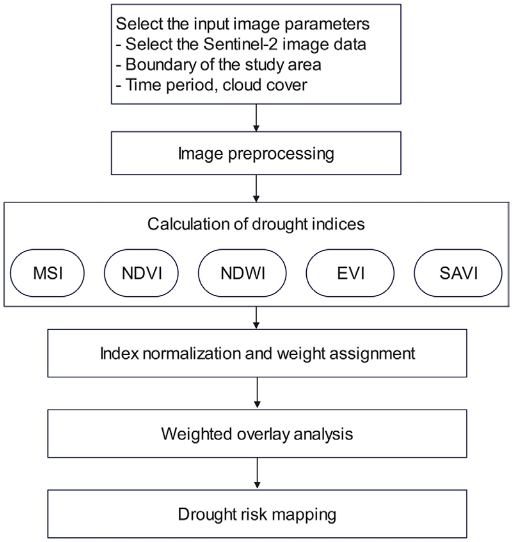

Figure 3: The flowchart of drought risk classification using Sentinel-2 imagery

Table 2: Vegetation and moisture indices for drought risk assessment using remote sensing

Index	Reference	Formula	Purpose	Range / Key Insights
EVI	Hunt and Rock (1989)	G × [(NIR – R) / (NIR + C1×R – C2×B + L)] where B2 = B, B4 = R, B8 = NIR, G = 2.5, C1 = 6, C2 = 7.5, L = 1	Improves sensitivity to canopy structure and reduces atmospheric influence.	Effective in areas with high biomass and dense vegetation cover.
MSI	Hunt and Rock (1989)	SWIR / NIR where B11 = SWIR, B8 = NIR	Identifies moisture stress levels in vegetation.	Higher values indicate increased vegetation water stress.
NDVI	Tucker (1979)	(NIR – R) / (NIR + R)	Indicates vegetation vigor and overall plant health.	Ranges from –1 to +1; higher values indicate healthier, denser vegetation.
NDWI	Gao (1996)	(NIR – SWIR) / (NIR + SWIR)	Detects vegetation water content and surface moisture availability.	Higher values suggest greater water availability in vegetation.
SAVI	Huete (1988)	[(NIR – R) × (1 + L)] / (NIR + R + L) with L = 0.5	Minimizes soil background effects in areas with sparse vegetation.	Useful in semi-arid regions or where vegetation cover is sparse.

Table 3: Classification criteria for hydrological drought risk assessment (Shinde and Telore, 2025)

Category	NDVI	NDWI	EVI	MSI	SAVI	Assigned risk value
Extreme drought	< 0.2	< -0.1	< 0.1	> 2.0	< -0.1	5
Severe drought	0.2 - 0.3	-0.1 - 0.0	0.1 - 0.15	1.5 - 2.0	-0.1 - 0.1	4
Moderate drought	0.3 - 0.4	0.0 - 0.1	0.15 - 0.2	1.0 - 1.5	0.1 - 0.2	3
Mild drought	0.4 - 0.5	0.1 - 0.2	0.2 - 0.25	0.5 - 1.0	0.2 - 0.3	2
No drought	> 0.5	> 0.2	> 0.25	< 0.5	> 0.3	1

To integrate diverse drought indicators into a unified risk assessment framework, each drought index was classified into five drought severity categories based on predefined threshold values. These thresholds were adopted from Shinde and Telore (2025) (Table 3), enabling a rule-based scoring approach that assigns each pixel a drought risk value from 1 (no drought) to 5 (extreme drought). The classification was implemented in Google Earth Engine using threshold-based conditional mapping with the *where()* and *remap()* functions.

Table 4. Weightage of vegetation and moisture indices for drought risk mapping (Shinde and Telore, 2025)

No.	Indicator	Weight (%)	Description
1	NDVI	30	Reflects vegetation vigor and is widely used to monitor agricultural drought conditions.
2	NDWI	25	Indicates surface water availability, serving as a key measure of hydrological drought.
3	EVI	20	Enhances detection of vegetation density and productivity under drought stress.
4	MSI	15	Detects moisture stress and dryness in vegetation and soil.
5	SAVI	10	Assesses vegetation health in sparsely vegetated or semi-arid areas.

Drought risk zone mapping was performed using a Weighted Overlay Analysis (WOA) that integrated five indicators: NDVI, NDWI, EVI, MSI, and SAVI. Each indicator was assigned a specific weight based on its relevance to different dimensions of drought (Shinde and Telore, 2025). NDVI, representing vegetation health and a proxy for agricultural drought, was given the highest weight (30%). NDWI, indicative of water availability and hydrological drought, received a weight of 25%. EVI, which enhances vegetation productivity detection under drought stress, was weighted at 20%. MSI, associated with moisture stress and soil dryness, was assigned a weight of 15%, while SAVI, suitable for assessing vegetation condition in areas with sparse cover, was weighted at 10%. NDVI was assigned the highest weight due to its strong linkage with vegetation vigor and agricultural drought, which is particularly relevant in Quang Tri province where rain-fed agriculture dominates and vegetation stress responds rapidly to moisture deficits. In contrast, SAVI received a lower weight because its primary advantage lies in reducing soil background effects, which are less influential in areas with relatively dense vegetation cover during the dry season. NDWI and MSI were incorporated to capture surface and vegetation moisture dynamics, while EVI was included to improve sensitivity under high biomass conditions. The integrated analysis allowed for a spatially explicit assessment of drought risk across the study area (Table 4).

To ensure the suitability of the classification and weighting scheme for local conditions, the criteria proposed by Shinde and Telore (2025) were first reviewed and then adapted to reflect the hydrological and climatic characteristics of Quang Tri province. A sensitivity analysis was conducted to assess how variations in index weights influence drought classification outcomes. The test involved adjusting each index weight by ±10% while maintaining the total weight at 100%. The results showed that spatial drought patterns remained largely stable, with only minor variations in drought extent (<5%), indicating the robustness of the adopted weighting scheme.

This classification allows for visualization and spatial analysis of drought risk distribution, which is essential for water resources planning, agricultural management, and climate adaptation strategies. Spatial visualization and analysis were performed in Google Earth Engine using map display and spatial aggregation functions, including *Map.addLayer()* and region-based reducers. Finally, the resulting datasets were exported to a local environment and further processed and cartographically refined in ArcGIS software. The map also provides a decision support tool for local authorities to prioritize areas for intervention, especially in areas that are frequently exposed to high drought stress during the period 2016-2025.

3 RESULTS AND DISCUSSION

The multi-temporal Sentinel-2 MSI satellite images covering the study area from 2016 to 2025 were preprocessed and clipped to the boundary of Quang Tri Province. The digital number (DN) values of the images were then converted to surface reflectance values for drought index calculation. From these surface reflectance images, five drought-related indices: NDVI, NDWI, EVI, MSI, and SAVI were systematically derived to capture both vegetation vigor and surface moisture dynamics across the study period. Figures 4-8 illustrate the spatial distribution and temporal variation of drought-related indices across Quang Tri province. Figures 4 and 6 show vegetation health and density through NDVI and EVI, Figure 5 presents vegetation and soil moisture stress indicated by MSI, Figure 7 displays surface water availability derived from NDWI, and Figure 8 highlights soil background effects and sparse vegetation conditions captured by SAVI.

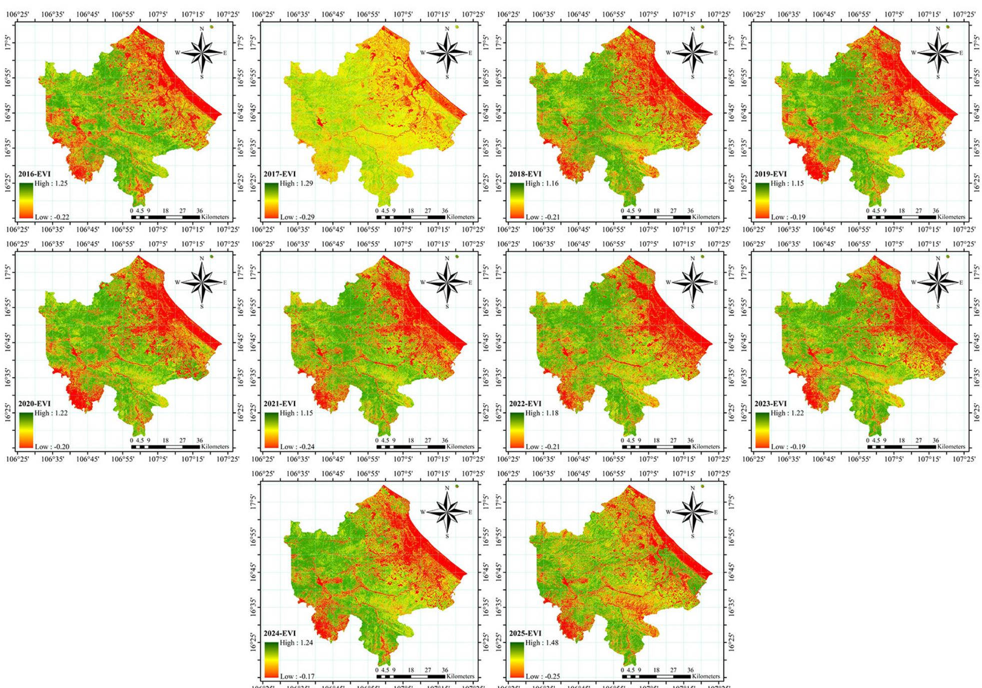

Figure 4: EVI images of the study area during the period 2016-2025

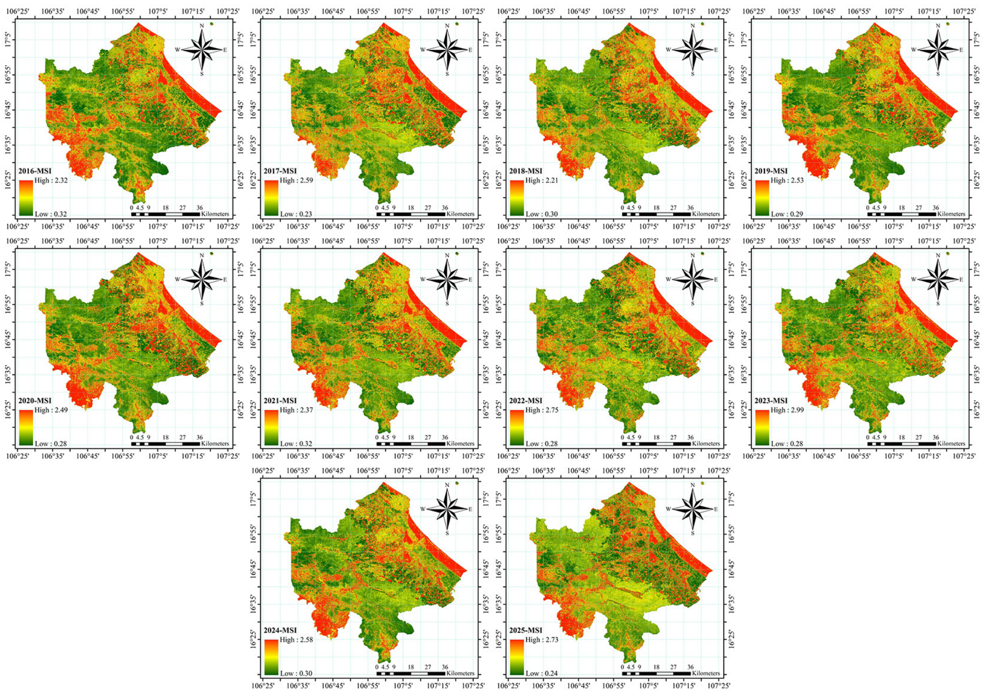

Figure 5: MSI images of the study area during the period 2016-2025

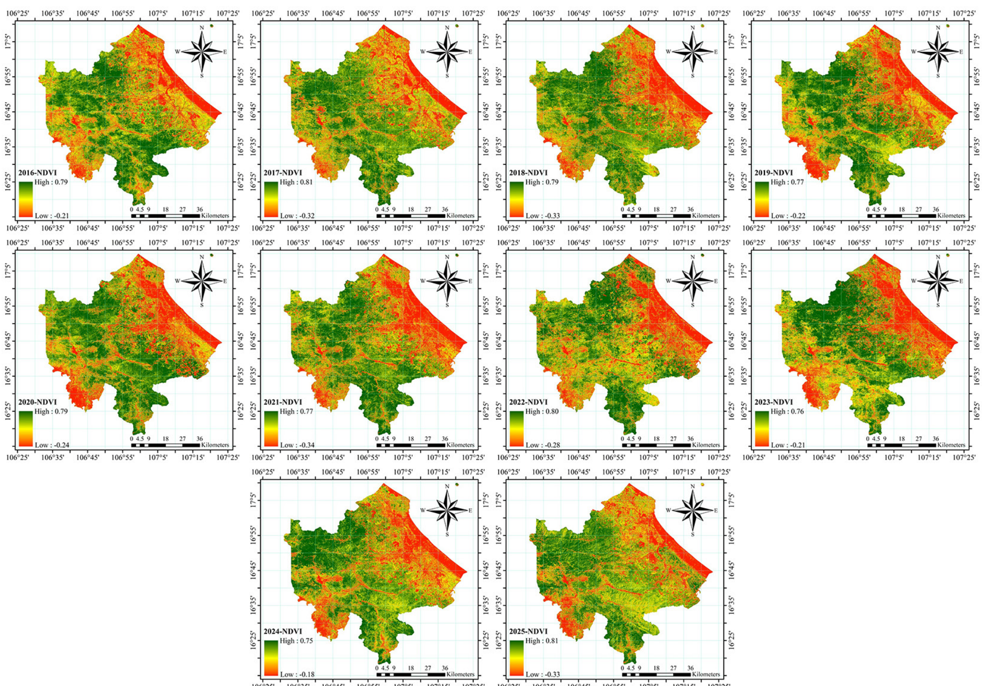

Figure 6: NDVI images of the study area during the period 2016-2025

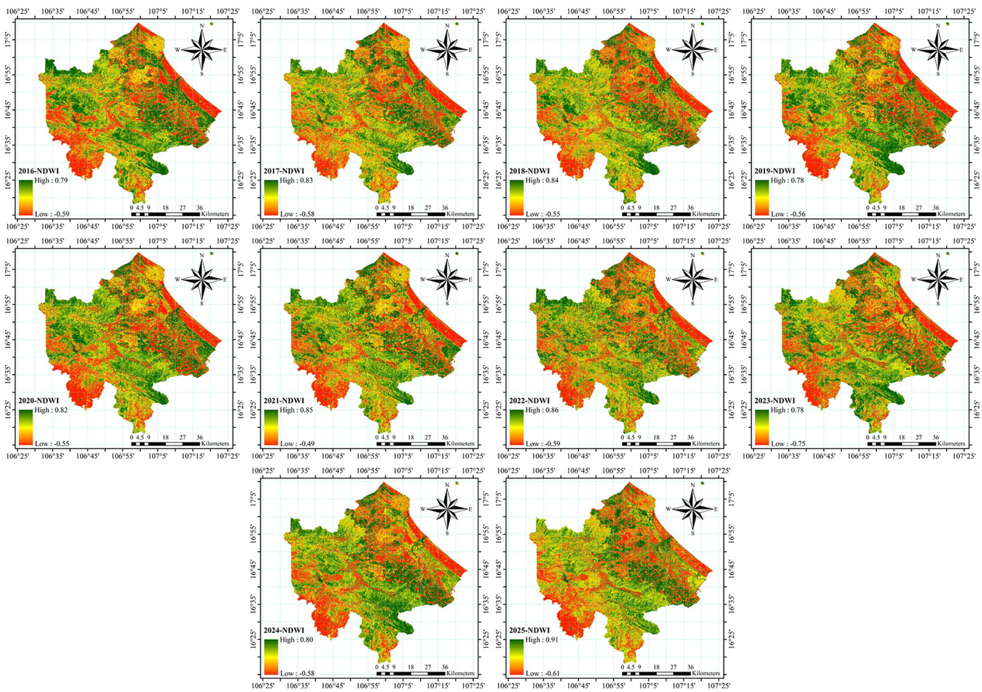

Figure 7: NDWI images of the study area during the period 2016-2025

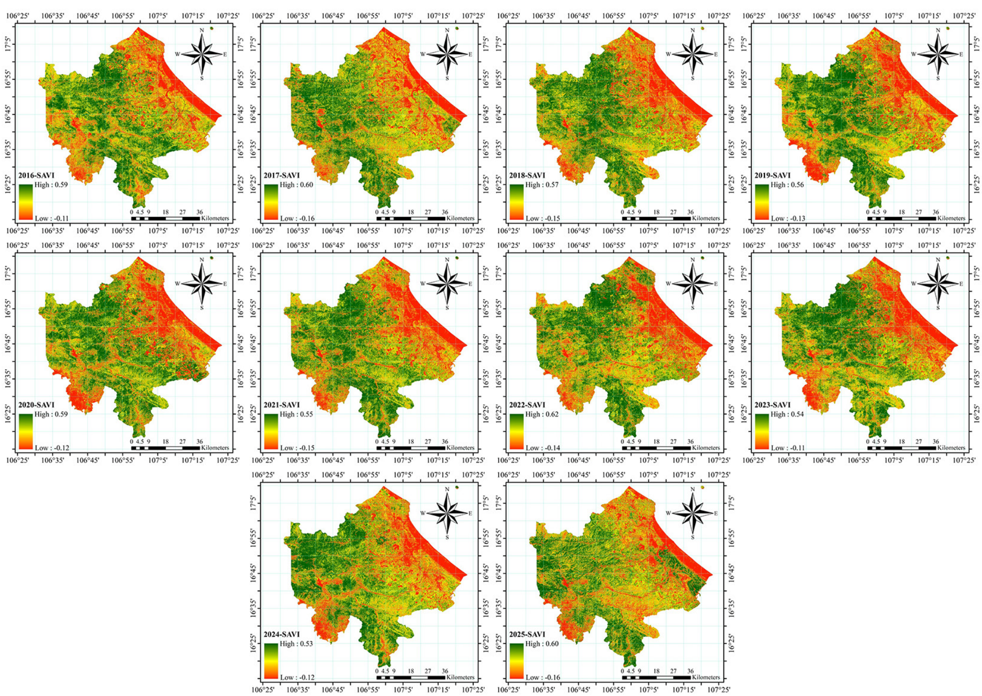

Figure 8: SAVI images of the study area during the period 2016-2025

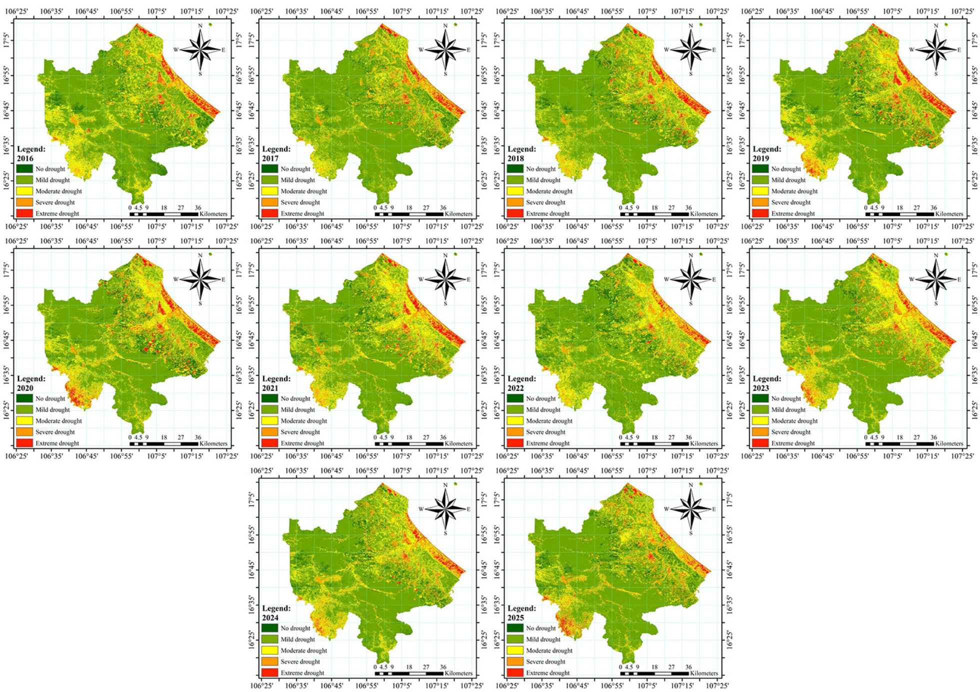

Figure 9: Drought risk maps of the study area during the period 2016-2025

Figure 9 presents the annual drought risk maps of Quang Tri province from 2016 to 2025, generated through the weighted integration of five drought-related indices. These maps highlight distinct spatial patterns of drought severity across the region. High-risk zones, classified as severe to extreme drought are predominantly concentrated in the eastern and northeastern coastal regions, where vegetation is sparse and surface water availability is limited.

In contrast, the central and western parts of the province, especially areas with dense forest cover and proximity to river systems, consistently exhibit lower drought risk (mild or no drought). Notably, some upland agricultural zones in the northeast frequently fall into the moderate-to-severe drought categories, indicating areas of concern for crop production. Meanwhile, the lowland plains in the south and southwest show more stable drought conditions over time, likely due to better irrigation and soil moisture retention. Overall, the maps illustrate the persistent vulnerability of coastal and upland zones, which should be prioritized in drought mitigation and land-use planning efforts.

To better understand the temporal and spatial distribution of drought severity in Quang Tri province from 2016 to 2025, the area and proportion of each drought level were analyzed based on the drought risk classification in Figure 10 and Table 5. First, during the 2016 - 2025 period, the area unaffected by drought exhibited significant fluctuations and a general downward trend. In 2016, the no drought zone covered 331.02 km², accounting for 6.83% of the total area. However, by 2023, this figure had dropped sharply to only 111.46 km² (2.30%), the lowest value recorded in the entire study period. Notably, a temporary increase in the no-drought area was observed in 2022, reaching 383.01 km² (7.90%), which deviates from the overall declining trend. This increase may be associated with enhanced precipitation during a weak La Niña phase. Nevertheless, the long-term reduction in no-drought areas suggests a progressive expansion of drought-affected zones and highlights increasing climatic variability across Quang Tri province.

Table 5: Area and proportion of drought severity levels in the study area during the period from 2016 to 2025

	No drought		Mild drought		Moderate drought		Severe drought		Extreme drought	
	km²	%	km²	%	km²	%	km²	%	km²	%
2016	331.02	6.83%	3087.95	63.72%	957.99	19.77%	350.95	7.24%	117.91	2.43%
2017	228.66	4.72%	3399.97	70.16%	746.65	15.41%	359.48	7.42%	111.06	2.29%
2018	229.43	4.73%	3315.41	68.42%	807.20	16.66%	358.42	7.40%	135.36	2.79%
2019	293.76	6.06%	3044.68	62.83%	904.84	18.67%	431.44	8.90%	171.10	3.53%
2020	287.77	5.94%	2914.37	60.14%	979.38	20.21%	476.96	9.84%	187.35	3.87%
2021	223.70	4.62%	3068.71	63.33%	1005.86	20.76%	403.96	8.34%	143.60	2.96%
2022	383.01	7.90%	3051.13	62.96%	973.15	20.08%	356.70	7.36%	81.83	1.69%
2023	111.46	2.30%	3195.24	65.94%	979.78	20.22%	432.12	8.92%	127.22	2.63%
2024	256.93	5.30%	3127.18	64.53%	930.06	19.19%	430.43	8.88%	101.22	2.09%
2025	264.67	5.46%	3209.18	66.23%	790.95	16.32%	454.12	9.37%	126.90	2.62%

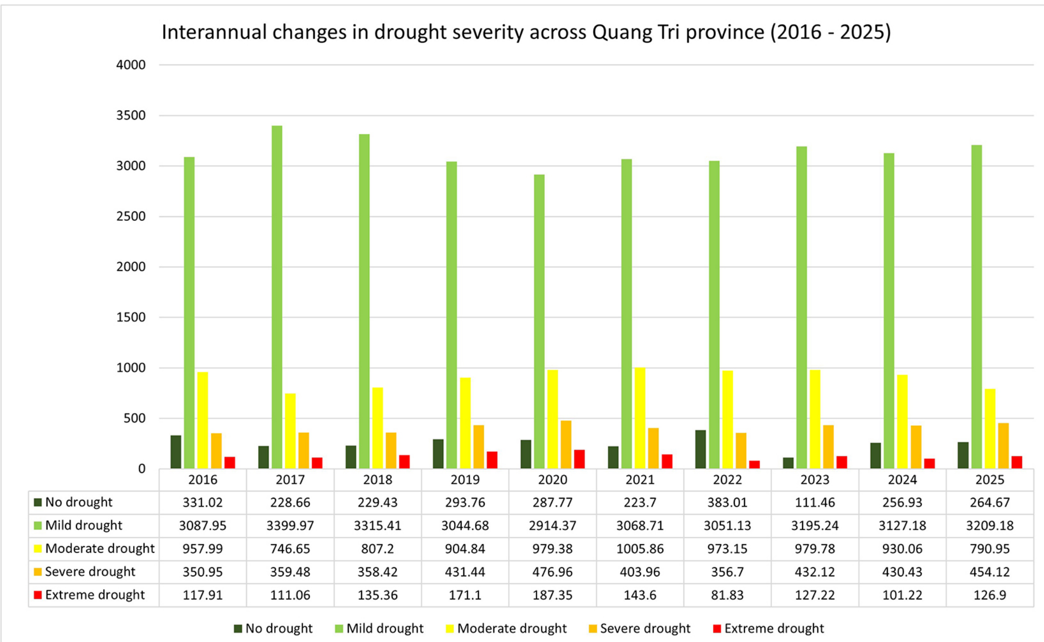

Figure 10: nterannual changes in drought severity across Quang Tri province (2016-2025)

In addition, mild drought was the most widespread severity level throughout the study period. The area affected by mild drought consistently occupied the largest proportion, ranging from 60.14% to 70.16% of the province. In 2017, the area under mild drought peaked at 3399.97 km² (70.16%). Although slight variations occurred in subsequent years, mild drought generally remained above 63 - 66%. This persistent condition indicates chronic soil moisture stress that can reduce yields, particularly in short-cycle crops such as peanuts and cassava. The widespread presence of mild drought highlights the need for adaptive farming practices, drought-tolerant crop varieties, and improved soil-water management to maintain productivity.

Moreover, moderate drought levels showed a slight upward trend between 2016 and 2022. The affected area ranged from 746.65 km² (15.41%) in 2017 to 1005.86 km² (20.76%) in 2021. From 2020 to 2022, the percentage of moderate drought stayed above 20%, indicating a concerning increase in moderate water stress conditions. Such drought intensity can influence rural livelihoods by increasing irrigation costs and groundwater extraction. Timely irrigation scheduling and sustainable water allocation policies are therefore essential to mitigate its socio-economic impacts.

Severe drought had a significant impact on ecosystems and agricultural activity during the study period. The year 2020 marked the peak, with 476.96 km² (9.84%) of the province experiencing severe drought. Neighboring years such as 2019 and 2021 also recorded high severe drought levels, with more than 400 km² affected. These years coincided with a strong El Niño event, likely intensifying evapotranspiration and surface dryness. Such conditions reduced crop productivity, accelerated soil degradation, and increased pressure on water resources. Although the area under severe drought slightly decreased after 2022, it remained higher than in the early years of the period (2016 - 2018), reflecting persistent and widespread dry conditions.

Extreme drought, the most critical category, affected a smaller area but posed serious threats. In 2020, the extreme drought area reached its highest level at 187.35 km² (3.87%). This year also marked the highest combined impact of both severe and extreme droughts, raising concerns about potential water crises and crop failure. While a slight decline in extreme drought area was observed in later years, it continued to range between 2% and 3%, particularly in vulnerable zones such as riverbanks, sandy soils, and barren lands with low moisture retention capacity. These extreme conditions have direct implications for food security and rural livelihoods. The spatial concentration of severe and extreme drought in central and western Quang Tri reflects vulnerability driven by both climate variability and land use change (for example, forest loss, agricultural expansion). Integrating drought monitoring with local water management, livelihood diversification, and climate adaptation strategies is essential to build long-term resilience.

Compared with the study by Tuan et al. (2014), which relied primarily on ground-based observations to assess temporal drought variability, the present study integrates satellite remote sensing data with field-based information to evaluate drought conditions across both spatial and temporal dimensions. Despite differences in data sources and methodological approaches, the two studies show consistent patterns in the identification and classification of drought severity levels in Quang Tri province, thereby reinforcing the reliability of the observed drought trends.

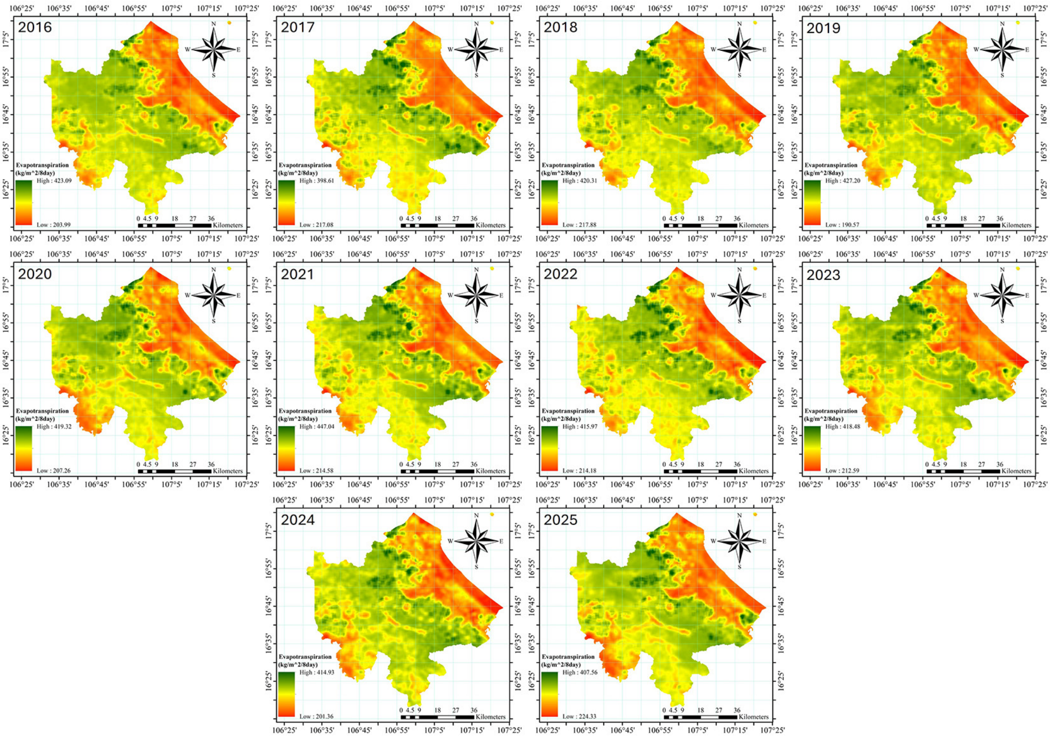

Figure 11: Evapotranspiration data for the study area during the period 2016-2025

Table 6: Correlation coefficient between evapotranspiration and drought severity levels for the period 2016-2025

Year	2016	2017	2018	2019	2020	2021	2022	2023	2024	2025
Correlation coefficient	-0.663	-0.562	-0.626	-0.666	-0.653	-0.634	-0.605	-0.643	-0.644	-0.630

The analysis of the correlation coefficient between evapotranspiration (ET) and drought severity levels in Quang Tri province for the period 2016-2025 reveals a clear inverse relationship, with coefficient values ranging from -0.562 to -0.666 (Figure 11 and Table 6). Evapotranspiration (ET) data were derived from the MOD16A2 MODIS product (8-day composite, 500 m spatial resolution), collected concurrently with the acquisition of Sentinel-2 imagery. This indicates that when drought severity increases, actual ET decreases due to lower soil moisture and reduced transpiration from vegetation; conversely, under more favorable moisture conditions, ET increases and drought severity decreases. This correlation remains relatively stable over the years, demonstrating that the drought severity analysis results are reliable for reflecting aridity conditions in the study area. The consistency between ET fluctuations and drought severity forecasts highlights the potential of applying remote sensing in drought monitoring systems, thereby enhancing early warning capabilities and supporting decision-making in water resource and agricultural management.

4 CONCLUSION

This study demonstrated the effectiveness of integrating Sentinel-2 surface reflectance imagery with a multi-index remote sensing approach to assess drought risk in Quang Tri province, Vietnam, during the period 2016 - 2025. By combining five drought-related indices (NDVI, NDWI, EVI, MSI, and SAVI) through a Weighted Overlay Analysis on the Google Earth Engine platform, spatially explicit drought risk maps were generated and classified into five severity levels. The results indicate that mild drought was the dominant condition throughout the study period, consistently accounting for approximately 60.14% - 70.16% of the provincial area, reflecting a persistent background level of soil moisture stress. More importantly, a substantial expansion of moderate to extreme drought was observed during 2020 - 2021, when severe drought peaked at 476.96 km² (9.84%) and extreme drought reached 187.35 km² (3.87%). This intensification coincided with a strong El Niño episode and was particularly pronounced in upland agricultural areas and coastal sandy zones characterized by sparse vegetation cover and low moisture retention capacity. These findings emphasize that drought risk in Quang Tri province is driven by the combined effects of large-scale climate variability, land-use characteristics, and topographic conditions, rather than climatic factors alone. From a practical perspective, the resulting drought risk maps provide a valuable decision-support tool for provincial authorities to prioritize irrigation management, crop structure adjustment, forest restoration, and targeted drought mitigation measures. Nevertheless, several limitations should be acknowledged, including uncertainties related to index threshold selection, weighting schemes, and the use of medium-resolution satellite data, which may not fully capture fine-scale soil moisture variability. Future studies should integrate meteorological, hydrological, and socio-economic datasets, as well as ground-based observations, to enhance the robustness of drought impact assessment and to support more comprehensive climate adaptation strategies.

Literature and references:

Agele, S. (2021). Global Warming and Drought, Agriculture, Water Resources, and Food Security: Impacts and Responses from the Tropics. In: Luetz, J.M., Ayal, D. (eds) Handbook of Climate Change Management. Springer, Cham. https://doi.org/10.1007/978-3-030-57281-5_183.

Arabzadeh, R., Kholoosi, M. M., & Bazrafshan, J. (2016). Regional hydrological drought monitoring using principal components analysis. Journal of Irrigation and Drainage Engineering, 142(1), 04015029. https://doi.org/10.1061/(ASCE)IR.1943-4774.0000925.

Baik, J., Park, J., Hao, Y. et al. (2022). Integration of multiple drought indices using a triple collocation approach. Stoch Environ Res Risk Assess 36, 1177–1195. https://doi.org/10.1007/s00477-021-02044-7.

Bogale, G. A., & Erena, Z. B. (2022). Drought vulnerability and impacts of climate change on livestock production and productivity in different agro-Ecological zones of Ethiopia. Journal of Applied Animal Research, 50(1), 471–489. https://doi.org/10.1080/09712119.2022.2103563.

Crocetti, L., Forkel, M., Fischer, M., Jurečka, F., Grlj, A., Salentinig, A. & Dorigo, W. (2020). Earth Observation for agricultural drought monitoring in the Pannonian Basin (southeastern Europe): current state and future directions. Regional Environmental Change, 20(4), 123. https://doi.org/10.1007/s10113-020-01710-w.

Diaz, V., Perez, G. A. C., Van Lanen, H. A., Solomatine, D., & Varouchakis, E. A. (2020). An approach to characterise spatio-temporal drought dynamics. Advances in Water Resources, 137, 103512. https://doi.org/10.1016/j.advwatres.2020.103512.

Gao, B. C. (1996). NDWI-A normalized difference water index for remote sensing of vegetation liquid water from space. Remote sensing of environment, 58(3), 257-266. https://doi.org/10.1016/S0034-4257(96)00067-3.

Gholinia, A., & Abbaszadeh, P. (2024). Agricultural Drought Monitoring: A Comparative Review of Conventional and Satellite-Based Indices. Atmosphere, 15(9), 1129. https://doi.org/10.3390/atmos15091129.

Ghosh, A., Mondal, M., Sarkar, D., & Nanda, M. K. (2024). Comparative study of remote sensing-derived indices for meteorological and agricultural drought monitoring: a review. Modern Cartography Series, 12, 381-412. https://doi.org/10.1016/B978-0-443-23890-1.00015-3.

Google Earth Engine. Harmonized Sentinel-2 MSI: MultiSpectral Instrument, Level-2A. https://developers.google.com/earth-engine/datasets/catalog/COPERNICUS_S2_SR_HARMONIZED, Accessed May 11, 2025.

Hodasová, K., Krčmář, D. & Ondrejková, I. (2025). Satellite-based drought assessment: integrating AHP method and fuzzy logic for comprehensive vulnerability and risk analysis. Nat Hazards 121, 11609–11632. https://doi.org/10.1007/s11069-025-07254-8.

Hollins, S., Dodson, J. (2013). Drought. In: Bobrowsky, P.T. (eds) Encyclopedia of Natural Hazards. Encyclopedia of Earth Sciences Series. Springer, Dordrecht. https://doi.org/10.1007/978-1-4020-4399-4_98.

Huete, A. R. (1988). A soil-adjusted vegetation index (SAVI). Remote sensing of environment, 25(3), 295-309. https://doi.org/10.1016/0034-4257(88)90106-X.

Hunt Jr, E. R., & Rock, B. N. (1989). Detection of changes in leaf water content using near-and middle-infrared reflectances. Remote sensing of environment, 30(1), 43-54. https://doi.org/10.1016/0034-4257(89)90046-1.

Kim, J. Kim E., Yu, J., Ryu, JH. et al. Assessment of regional drought vulnerability and risk using principal component analysis and a Gaussian mixture model. Nat Hazards 109, 707–724 (2021). https://doi.org/10.1007/s11069-021-04854-y.

Kumar, V., Sharma, K. V., Pham, Q. B., Srivastava, A. K., Bogireddy, C., & Yadav, S. M. (2024). Advancements in drought using remote sensing: assessing progress, overcoming challenges, and exploring future opportunities. Theoretical and Applied Climatology, 155(6), 4251-4288. https://doi.org/10.1007/s00704-024-04914-w.

Maybank, J., Bonsai, B., Jones, K., Lawford, R., O'Brien, E. G., Ripley, E. A., & Wheaton, E. (1995). Drought as a natural disaster. Atmosphere-Ocean, 33(2), 195-222. https://doi.org/10.1080/07055900.1995.9649532.

Mishra, A. K., Singh, V. P. (2010). A review of drought concepts. Journal of hydrology, 391(1-2), 202-216. https://doi.org/10.1016/j.jhydrol.2010.07.012.

Moskolaï, W. R., Abdou, W., Dipanda, A., & Kolyang. (2021). Application of Deep Learning Architectures for Satellite Image Time Series Prediction: A Review. Remote Sensing, 13(23), 4822. https://doi.org/10.3390/rs13234822.

Mullapudi, A., Vibhute, A.D., Mali, S. et al. (2023). A review of agricultural drought assessment with remote sensing data: methods, issues, challenges and opportunities. Appl Geomat 15, 1-13 (2023). https://doi.org/10.1007/s12518-022-00484-6.

Orimoloye, I. R., Belle, J. A., Orimoloye, Y. M., Olusola, A. O., & Ololade, O. O. (2022). Drought: A Common Environmental Disaster. Atmosphere, 13(1), 111. https://doi.org/10.3390/atmos13010111.

Prodhan, F. A., Zhang, J., Yao, F., Shi, L., Pangali Sharma, T. P., Zhang, D., Cao, D., Zheng, M., Ahmed, N., & Mohana, H. P. (2021). Deep Learning for Monitoring Agricultural Drought in South Asia Using Remote Sensing Data. Remote Sensing, 13(9), 1715. https://doi.org/10.3390/rs13091715.

Pelletier, C., Webb, G. I., & Petitjean, F. (2019). Temporal Convolutional Neural Network for the Classification of Satellite Image Time Series. Remote Sensing, 11(5), 523. https://doi.org/10.3390/rs11050523.

Prodhan, F. A., Zhang, J., Hasan, S. S., Sharma, T. P. P., & Mohana, H. P. (2022). A review of machine learning methods for drought hazard monitoring and forecasting: Current research trends, challenges, and future research directions. Environmental modelling & software, 149, 105327.

Pulwarty, R. S., & Sivakumar, M. V. (2014). Information systems in a changing climate: Early warnings and drought risk management. Weather and Climate Extremes, 3, 14-21. https://doi.org/10.1016/j.wace.2014.03.005.

Shinde Prakash, S., & Telore Namdev, V. (2025). Drought Risk Assessment in the Yerla River Basin of India using Remote Sensing and GIS Methods. Disaster Advances; Vol. 18(4); 30-36; doi: https://doi.org/10.25303/184da030036.

The European Space Agency (ESA). Overview of Sentinel-2 Mission. https://sentiwiki.copernicus.eu/web/s2-mission, Accessed May 11, 2025.

The European Space Agency (ESA). (2013). Sentinel-2 User Handbook. Accessed May 13, 2025.

The European Space Agency (ESA). Sentinel Online. https://sentinel.esa.int/, Accessed May 13, 2025.

Trinh, L. H. & Vu, D. T. (2019). Application of remote sensing technique for drought assessment based on normalized difference drought index, a case study of Bac Binh district, Binh Thuan province (Vietnam). Russian Journal of Earth Sciences, 19, ES2003, doi:10.2205/2018ES000647.

Tuan, D. D., Van Hoang, N., & Van Loi, N. (2014). Study of climatic drought status in Quang Tri Province. Vietnam Journal of Earth Sciences, 36(2), 160-168.

Tucker, C. J. (1979). Red and photographic infrared linear combinations for monitoring vegetation. Remote sensing of Environment, 8(2), 127-150. https://doi.org/10.1016/0034-4257(79)90013-0.

Tyagi, S., Zhang, X., Saraswat, D., Sahany, S., Mishra, S. K., & Niyogi, D. (2022). Flash drought: Review of concept, prediction and the potential for machine learning, deep learning methods. Earth's Future, 10(11), e2022EF002723. https://doi.org/10.1029/2022EF002723.

Van Loon, A. F. (2015). Hydrological drought explained. Wiley Interdisciplinary Reviews: Water, 2(4), 359-392. https://doi.org/10.1002/wat2.1085.

Vogt, J.V., Naumann, G., Masante, D., Spinoni, J., Cammalleri, C., Erian, W., Pischke, F., Pulwarty, R., Barbosa, P. (2018). Drought Risk Assessment. A conceptual Framework. EUR 29464 EN, Publications Office of the European Union, Luxembourg, 2018. ISBN 978-92-79-97469-4, doi:10.2760/057223, JRC113937.

Wang, W., & Wang, H. (2025). Rethinking drought definition and classification. Water Science and Engineering. https://doi.org/10.1016/j.wse.2025.04.002.

Wang, X., Zhang, J., Xun, L., Wang, J., Wu, Z., Henchiri, M., Zhang, S., Zhang, S., Bai, Y., Yang, S., Li, S., & Yu, X. (2022). Evaluating the Effectiveness of Machine Learning and Deep Learning Models Combined Time-Series Satellite Data for Multiple Crop Types Classification over a Large-Scale Region. Remote Sensing, 14(10), 2341. https://doi.org/10.3390/rs14102341.

Wilhite, D.A. (Ed.). (2000). Droughts: A Global Assesment (1st ed.). Routledge. https://doi.org/10.4324/9781315830896.

Trinh L. H., Tran T. T. T., Le V. P., Do T. P. T., Tong T. H. (2026). Application of remote sensing in drought risk assessment using spectral indices and modelling: a case study in North Central Vietnam. Geodetski vestnik, 70 (2), 213-229.
DOI: https://doi.org/geodetski-vestnik.2026.02.213-229

Le Hung TRINH, Associate Prof., Ph.D.
Le Quy Don Technical University,
236 Hoang Quoc Viet Str., Hanoi, Vietnam;
e-mail: trinhlehung@lqdtu.edu.vn

Thi Thu Trang TRAN, Master of Technical Sciences
Hanoi University of Mining and Geology,
Hanoi, Vietnam;
e-mail: tranthithutrang@humg.edu.vn

Thi Phuong Thao DO, Ph.D.
Hanoi University of Mining and Geology,
Hanoi, Vietnam;
dothiphuongthao@humg.edu.vn

Van Phu LE, Master of Technical Sciences,
Le Quy Don Technical University,
236 Hoang Quoc Viet Str., Hanoi, Vietnam;
e-mail: phule.ktqs.53@gmail.com

Thi Hanh TONG, Master of Technical Sciences
Le Quy Don Technical University,
236 Hoang Quoc Viet Str., Hanoi, Vietnam;
e-mail: hanhkhuenam@gmail.com